Available online at www.sciencedirect.com
SCIENCE DIRECT®
Journal of Molecular Catalysis A: Chemical 221 (2004) 209–221
JOURNAL OF MOLECULAR CATALYSIS A: CHEMICAL
www.elsevier.com/locate/molcata

Optical and catalytic properties of Ag_2S nanoparticles

A.I. Kryukov, A.L. Stroyuk*, N.N. Zin'chuk, A.V. Korzhak, S.Ya. Kuchmii

L.V. Pysarzhevsky Institute of Physical Chemistry, National Academy of Sciences of Ukraine, 31 Prosp. Nauky, 03028 Kyiv, Ukraine

Received 14 June 2004; received in revised form 9 July 2004; accepted 10 July 2004
Available online 25 August 2004

Abstract

Optical properties of polymer-stabilized aqueous colloids of silver sulfide were studied. Nature and energies of optical transitions responsible for the absorption of visible light by silver sulfide nanoparticles were determined. Catalytic properties of Ag_2S nanoparticles in methylviologen reduction by sodium sulfide were examined. It was shown that this reaction is reversible, the equilibrium caused by a reverse reaction between the product of direct catalytic process – sulfur (polysulfide anions) and cation-radical of methylviologen. It was found that Ag_2S nanoparticles can catalyze reduction of Ag^+ ions by various reductants, in particular, hydroquinone or sodium sulfite, with the formation of silver particles having characteristic plasmon absorption bands in the visible spectral domain. Effect of the conditions of Ag^+ catalytic reduction on the shape and intensity of plasmon resonance bands of metallic silver were studied, schematic mechanism of this reaction was proposed. It was shown that at the irradiation of solutions containing Ag_2S nanoparticles, Ag^+ cations and a reducing agent with the light corresponding to the fundamental absorption band of nanoparticulate silver sulfide, the rate of Ag^+ catalytic reduction increased whereas kinetic features of catalytic reaction and characteristics of plasmon resonance absorption bands of silver nanoparticles changed. A mechanism of photochemical activation of the catalytic reduction of silver ions with the participation of Ag_2S nanoparticles was proposed.
© 2004 Elsevier B.V. All rights reserved.

Keywords: Silver sulfide nanoparticles; Silver nanoparticles; Methylviologen; Catalytic reduction; Photochemical activation

1. Introduction

Synthesis, properties and application potential of semiconductor nanoparticles manifesting photocatalytic activity in various redox-processes have been and are the subject of great interest to the present day [1–9]. On the other hand nanoparticles of a large group of semiconductors, which have not been yet used as photocatalysts or electrodes in photoelectrochemical systems remained to date virtually beyound the scope of research. At the same time small particles or monolayer fragments of the semiconductors of this group deposited on the surface of semiconductor photocatalysts are found to increase the photoactivity of the substrate or to expand its photosensitivity to visible domain of the spectrum [1,10]. Silver sulfide is one of the semiconductors which in nanoparticulate state can strongly affect in that way the functioning of various light-sensitive systems. It was shown that deposition of Ag_2S nanoparticles onto the surface of electrodes made of porous titanium dioxide caused a shift of "red" edge of the photosensitivity of the substrate from 400 nm to near infrared part of the spectrum [11]. It is known that silver sulfide can sensitize photographic materials [12,13], form self-assembled layers of nanoparticles [14] and change luminescence properties of cadmium sulfide nanoparticles [15]. It was also noticed that silver sulfide can be potentially used for photography and photodetection in infrared region [16]. At the same time, among the numerous publications concerning nanometer semiconductor particles including silver sulfide nanoparticles we did not find examples of the possibility of the participation of Ag_2S nanoparticles in thermal ("dark") processes, i.e. in reactions not demanding the irradiation, especially as a catalyst.

The subjects of the present paper are optical properties of Ag_2S aqueous colloidal solutions and catalytic activity

* Corresponding author. Tel.: +38 44 265 0270.
E-mail addresses: stroyuk@inphyschem-nas.kiev.ua, photochem@ukrpost.net (A.L. Stroyuk).

1381-1169/$ – see front matter © 2004 Elsevier B.V. All rights reserved.
doi:10.1016/j.molcata.2004.07.009

of silver sulfide nanoparticles in two reactions proceeding in the dark (without absorption of light quanta), namely, in methylviologen and Ag^+ ions reduction. It was shown that the efficiency of the second reaction can be substantially increased by the irradiation of reacting mixtures with the light, corresponding to the absorption band of Ag_2S nanoparticles.

2. Experimental

For the preparation of stock solutions we used commercial silver nitrate, sodium sulfite, hydroquinone, methylviologen dichloride (Aldrich) and sodium sulfide (Aldrich) of reagent grade quality without additional purification. Ag_2S nanoparticles were synthesized via successive addition of aliquots of silver nitrate and sodium sulfide stock solutions to a solution of a stabilizer. Polyvinyl alcohol (PVA) and gelatine were used as stabilizers. In a series of experiments Ag_2S nanoparticles were synthesized without the addition of stabilizers. At $[Ag_2S] \leq 1 \times 10^{-3}$ M such solutions are transparent, do not scatter light and remain stable over many hours, while in more concentrated solutions precipitation of silver sulfide begins almost at once after the preparation of the colloidal solution. Colloidal solutions of silver sulfide stabilized with PVA or gelatine do not noticeably change their properties while kept at room temperature for several months.

Kinetic measurements were conducted in thermostatically controlled glass reactors at 20–25 °C in air-saturated solutions. Reaction rates were determined from the absorption spectra of the reacting mixtures.

3. Discussion

3.1. Optical properties of Ag_2S nanoparticles

Absorption spectra of colloidal silver sulfide prepared at various conditions are given in Fig. 1. Regardless of the synthetic procedure and conditions of stabilization of colloidal silver sulfide, its absorption spectra in the 250–750 nm region are represented by curves monotonously rising towards the short-wave side. Absence of distinctly prononced edge of the absorption bands as well as maxima or elbows on spectral curves complicates extraction of the information about photophysical properties of Ag_2S nanoparticles or their energetic characteristics directly from absorption spectra. So, for the elucidation of the nature of primary photoprocesses in Ag_2S nanoparticles we performed an analysis of absorption spectra of colloidal silver sulfide using the conceptions of the optics of semiconductors.

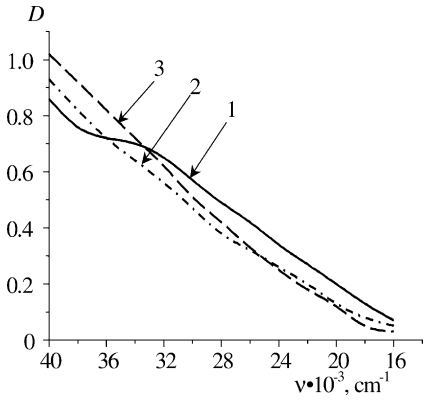

Fig. 1. Electronic absorption spectra of Ag_2S nanoparticles synthesized in the absence of stabilizers (curve 1), in the presence of PVA, 2.5 mass% (curve 2), in the presence of gelatine, 0.5 mass% (curve 3). $[Ag_2S] = 5 \times 10^{-4}$ M, optical path $l = 0.2$ cm.

According to the theory of optical transitions in semiconductors [17], light absorption can lead both to direct (vertical) interband transitions and indirect electronic transitions, the latters occuring with the participartion of energy quanta of lattice oscillations (phonons). Band gap of a semiconductor (E_g), energy of light quanta ($E_{h\nu}$), absorption coefficients corresponding to direct (α_d) and indirect (α_i) transitions as well as corresponding absorption constants (B_d, B_i) are related with each other via following expressions:

$$\alpha_d = \frac{B_d(E_{h\nu} - E_g)^{0.5}}{E_{h\nu}} \quad (1)$$

$$\alpha_i = \frac{B_i(E_{h\nu} - E_g)^2}{E_{h\nu}} \quad (2)$$

Linearity of a spectral curve in $(\alpha E_{h\nu})^2 - E_{h\nu}$ coordinates indicates direct interband optical transition whereas in $(\alpha E_{h\nu})^{1/2} - E_{h\nu}$ coordinates indirect transitions. Extrapolation of linear section of the corresponding anamorphosis to the abscissa axis gives the value of $E_{h\nu} = E_d = E_g$ in case of direct transitions or $E_{h\nu} = E_i = E_g + E_f$ in case of indirect transitions (where E_f is the energy of phonon participating in a transition).

We used Eqs. (1) and (2) for determination of type and energies of electronic transitions in synthesized colloidal Ag_2S nanoparticles. Absorption coefficients (in cm^{-1}) were calculated using the following equation:

$$\alpha = 2.303 \times 10^3 D\rho(lc)^{-1} \quad (3)$$

where D is the optical density of a solution, ρ the density of bulk Ag_2S (7.2 g cm^{-3}), l the optical thickness of a cuvette (cm), c the concentration of a colloidal solution (g l^{-1}).

Energetic dependences of absorption coefficient, calculated for colloidal Ag_2S solutions synthesized in different conditions are shown in Fig. 2. It can be seen that in all cases both direct and indirect electronic transitions can occur at the photoexcitation of silver sulfide nanoparticles. From the results of the calculation of transitions energies (Table 1) a number of additional conclusions about the primary photoprocesses in synthesized semiconductor materials can be derived. As can be concluded from Table 1, energies of optical transitions in Ag_2S nanoparticles exceed the same values of bulk crystals of silver sulfide (for bulk Ag_2S $E_g = 0.9$ eV

Table 1
Energies of indirect (E_i) and direct (E_d) optical interband transitions in Ag_2S nanoparticles

No.	[Ag_2S] (M)	Stabilization conditions	Indirect transitions	Direct transitions	$E_d - E_i$ (eV)
			E_i (eV)	E_d (eV)	
1	1.0×10^{-3}	Without stabilizer	1.00 1.36	2.66	1.66
2	5.0×10^{-4}	Without stabilizer	0.98 1.44	3.10 3.60	1.66
3	1.0×10^{-4}	Without stabilizer	1.10 1.36	2.86 3.20	1.76 1.74
4	5.0×10^{-3}	PVA, 2.5%	0.96 1.44		
5	2.0×10^{-3}	Without stabilizer	1.15 1.60	3.36	1.76
6	5.0×10^{-4}	Without stabilizer	0.96 1.66	3.34 3.68	1.68
7	2.0×10^{-4}	Without stabilizer	1.24 1.66	3.35 3.70	1.69
8	1.0×10^{-4}	Without stabilizer	1.10 1.58	3.28 3.78	1.70
9	7.0×10^{-5}	Without stabilizer	1.54	3.20 4.04	1.66
10	6.2×10^{-5}	Without stabilizer	1.10 1.60	3.32 4.00	1.72
11	5.0×10^{-3}	Gelatine, 0.25%	1.00 1.60		
12	1.0×10^{-3}	Without stabilizer	1.18 1.76	3.50 3.96	1.74
13	5.0×10^{-4}	Without stabilizer	0.90 1.74	3.44	1.70

[18]). Hence, synthesized colloidal nanoparticles manifest quantum confinement effects lying in a variation of band gap of the semiconductor with a change in the size of nanocrystals [6–8]. These effects can be observed especially clearly in case of high-energy indirect transition. Thus, in non-stabilized colloidal solution (containing the biggest of all synthesized Ag_2S particles), energy of indirect transition (E_i) was found to be close to 1.4 eV (see Table 1, rows 1–3), while in case of PVA-stabilized solutions is close to 1.6 eV (Table 1, rows 4–10). Smaller Ag_2S particles with more prononced quantum confinement effect which have $E_i = 1.70 – 1.76$ eV can be formed in gelatine-stabilized solutions (Table 1, rows 11–13). Concentration of solutions do not affect so strongly the process of particles formation as the nature and concentration of a stabilizer. Only in case of poorly stable solutions with the concentration of Ag_2S as large as 5×10^{-3} M in the presence of PVA we obtained the value of $E_i = 1.44$ eV (Table 1, row 4), which distinctly differs from the same value calculated for the solutions with Ag_2S concentration in the range of 7×10^{-5} to 2×10^{-3} M, whereas in the presence of gelatine $E_i = 1.60$ eV (Table 1, row 11).

Along with discussed indirect transitions in silver sulfide nanoparticles having average size and dominating in colloidal solutions, analysis of absorption spectra revealed for each sample the possibility of transitions that are also indirect but have lower energy. We suppose that these transitions correspond to a fraction of colloidal Ag_2S particles of the greatest size. Absorption band of these nanoparticles do not substantially overlap with the band of adjacent fractions of nanoparticles, so even at very small concentration of such particles it is possible to observe distinct linear section of $(\alpha E_{h\nu})^{1/2} - E_{h\nu}$ dependence and determine E_i value (see Fig. 2). The values of the energies of these transitions listed in Table 1 should be considered as rough estimation since these values can be strongly distorted owing to very small content of such particles in solutions as well as light absorption due to intraband transitions.

Analyzing the absorption spectra in UV region we found that the majority of examined samples have one or two direct interband electronic transitions. At the examination of experimental results (Table 1) our attention was drawn by direct transitions at 3.10–3.50 eV, the precise value of energy varying depending on the conditions of stabilization. In case of non-stabilized colloids we obtained the E_d equal to 3.10 and 3.20 eV, for PVA-stabilized Ag_2S nanoparticles close to 3.3 eV, and for gelatine-stabilized particles near 3.5 eV.

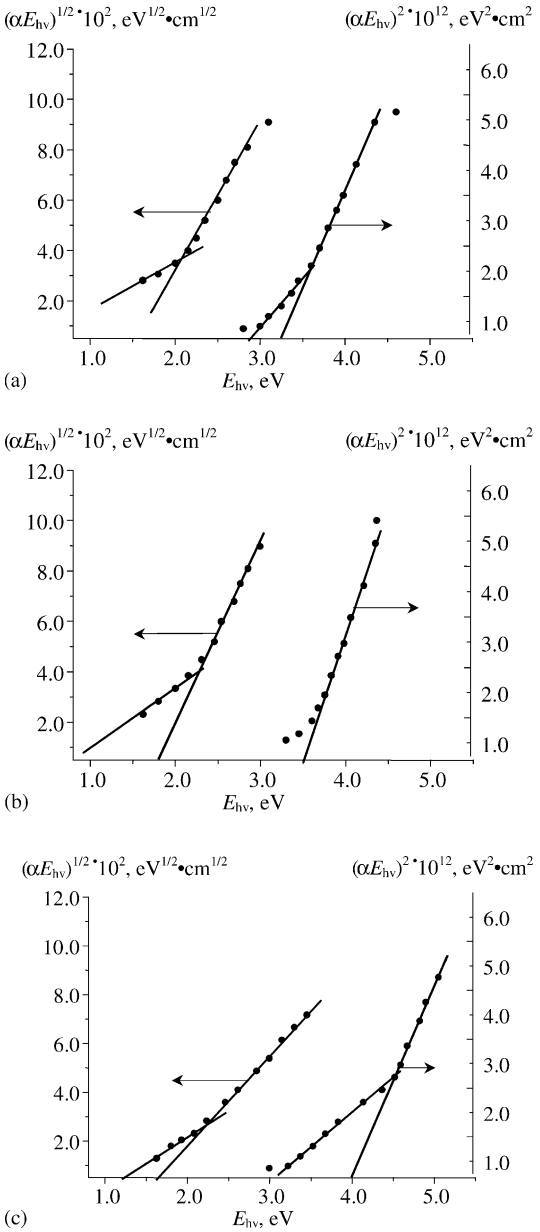

Fig. 2. Dependences $(\alpha E_{h\nu})^{1/2} - E_{h\nu}$ and $(\alpha E_{h\nu})^2 - E_{h\nu}$ for Ag_2S nanoparticles synthesized (a) in the absence of stabilizers at $[Ag_2S] = 5 \times 10^{-4}$ M, (b) in the presence of 0.25% gelatine, $[Ag_2S] = 5 \times 10^{-4}$ M; (c) in the presence of 2.5% PVA, $[Ag_2S] = 1 \times 10^{-3}$ M.

Comparison of these values with the energies of indirect transitions in Ag_2S nanoparticles of an average size showed that in all cases an energy gap between them remains virtually constant, i.e. $E_d - E_i \approx 1.7$ eV. It follows from this that transitions of both types are excited in the same particles having an average size. As can be seen from Table 1 (rows 1 and 3) the same values of $E_d - E_i$ were obtained in case of the biggest nanoparticles formed in non-stabilized solutions. Hence, quantum confinement effect in Ag_2S nanoparticles apparently do not affect reciprocal disposition of energy levels participating in these transitions.

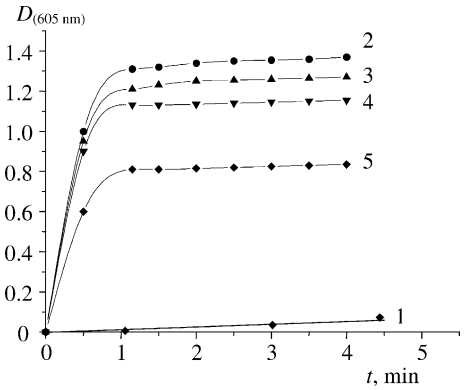

Fig. 3. Kinetic curves of the accumulation of methylviologen cation-radical ($MV^{\bullet+}$) in solutions containing sodium sulfide in the absence of Ag_2S nanoparticles (1), in the presence of Ag_2S nanoparticles (2), in the presence of Ag_2S nanoparticles and sodium polysulfide—$[Na_2S_x] = 4.0 \times 10^{-3}$ M (3), 5.0×10^{-3} M (4), 8.0×10^{-3} M (5). $[Ag_2S] = 5 \times 10^{-4}$ M, $[Na_2S] = 1 \times 10^{-2}$ M, $[MV^{2+}] = 1 \times 10^{-3}$ M. Concentration of PVA: 2.5 mass%.

3.2. Ag_2S nanoparticles as the catalyst of methylviologen reduction

One-electron reduction of methylviologen bication results in the formation of cation-radical $MV^{\bullet+}$ having absorption band in the visible spectral domain (λ_{max} = 605 nm and molar extinction coefficient in maximum ε_{605} = 13,700 M^{-1} cm^{-1} [1,19]). So, the process of reduction can be easily monitored by the evolution of the absorption band of cation-radical. As can be seen in Fig. 3, methylviologen reduction by sodium sulfide which is quite slow process in aqueous solutions in the absence of additional catalysts, can be substantially accelerated in the presence of silver sulfide nanoparticles. However, high initial rate of the reaction observed after reagents mixing rapidly decreases and after 5–10 min growth of the intensity of the absorption band of $MV^{\bullet+}$ cation-radical becomes almost imperceptible. The concentration of cation-radical reached at this stage do not change further at prolonged ageing of reacting mixtures and is thereby very close to maximal. It was also found that the reaction do not finish due to full consumption of reagents but reach certain equilibrium state. For example, in case depicted by the curve 4 in Fig. 3, about 10% of MV^{2+} and 0.2% of two-electron reductant (sodium sulfide) were consumed before an equilibrium state was reached. The equilibrium can be caused by the accumulation of a product of the reduction, in particular, polysulfide-ions:

$$MV^{2+} + HS^- \rightarrow MV^{\bullet+} + HS^{\bullet} \quad (4)$$

$$MV^{2+} + HS^{\bullet} \rightarrow MV^{\bullet+} + S^0 + H^+ \quad (5)$$

$$HS^- + (x-1)S^0 \rightarrow S_x{}^{2-} + H^+ \quad (6)$$

As can be seen in Fig. 3 (curves 3–5), addition of polysulfide ions to a reacting mixture actually causes both fall of the rate of catalytic reduction of methylviologen and a decrease in the maximal yield of $MV^{\bullet+}$ cation-radical. Recommencement of fast reaction at the introduction of

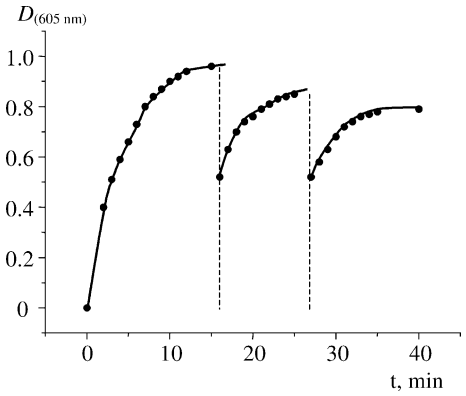

Fig. 4. Accumulation of methylviologen cation-radical in air-saturated solutions containing sodium sulfide and Ag_2S nanoparticles. Dotted lines correspond to the moments of the stirring. $[Ag_2S] = 5 \times 10^{-4}$ M, $[Na_2S] = 1 \times 10^{-2}$ M, $[MV^{2+}] = 1 \times 10^{-3}$ M. PVA concentration: 2.5 mass%.

additional amounts of Na_2S or MV^{2+} into the reacting system where the accumulation of $MV^{\bullet+}$ has previously stopped, directly indicates that Ag_2S nanoparticles do not lose their ability to accelerate reduction, i.e. to be the catalyst of methylviologen reduction.

At intense stirring of air-saturated solutions rapid decoloration is observed due to $MV^{\bullet+}$ oxidation by O_2, then reduction recommences again (Fig. 4). Such cyclic MV^{2+} reduction–$MV^{\bullet+}$ oxidation can repeat many times. At that redox-potential of $MV^{2+}/MV^{\bullet+}$ couple first approaches to redox-potential of S^0/HS^- couple up to some equilibrium state and then, in the result of irreversible reaction between the cation-radical and oxygen, rapidly returns to the initial value. Since the value of $E(S^0/HS^-)$ changes at that irreversibly due to the accumulation of S_x^{2-} ions, both the rate and maximal yield of $MV^{\bullet+}$, as can be seen in Fig. 4, decrease at every regeneration of methylviologen bication.

The rate (dx/dt) and equilibrium constant (K) of catalytic methylviologen reduction, which can be described by brutto-equation (7) can be determined from the Eqs. (8) and (9) correspondingly:

$$2MV^{2+} + S^{2-} \leftrightarrow 2MV^{\bullet+} + S^0 \tag{7}$$

$$\frac{dx}{dt} = k_1([MV^{2+}]_0 - x)^2([S^{2-}]_0 - x) - k_2([MV^{\bullet+}]_0 + x)^2([S^0]_0 + x) \tag{8}$$

$$K = \frac{([MV^{\bullet+}]_0 + x_{eq})^2([S^0]_0 + x_{eq})}{([S^{2-}]_0 - x_{eq})([MV^{2+}]^0 - x_{eq})^2} \tag{9}$$

where $x = ([MV^{\bullet+}] - [MV^{\bullet+}]_0)/2$, $[MV^{\bullet+}]_0$ $[S^{2-}]^0$, $[S^0]_0$ are the molar concentrations of cation radical of methylviologen, sulfide ions and elemental sulfur (in the form of polysulfide ions) at the moment when the reduction starts, k_1, k_2 the rate constants of the direct and reverse reactions correspondingly, x_{eq} the x value in an equilibrium state.

Values of K calculated for the systems with different concentration of polysulfide-ions (see Fig. 3) are listed in Table 2. Calculations were performed with experimental values of x_{eq} assuming $[MV^{\bullet+}]_0 = 0$. In the experiments on the effect of polysulfide addition on the rate of catalytic reaction the following conditions were kept: $[S^{2-}]_0 \gg x$, $[MV^{2+}]_0 \gg x$, $[S^0]_0 \gg x$ and $[MV^{\bullet+}]^0 = 0$, so Eq. (8) can be simplified as follows:

$$\frac{dx}{dt} = k_1[MV^{2+}]_0^2[S^{2-}]_0 - k_2x^2[S^0]_0 \tag{10}$$

In an equilibrium state the rate of direct and reverse reactions are equal, so we can calculate the ratio of rate constants k_1 and k_2 (see Table 2):

$$k_1[MV^{2+}]_0^2[S^{2-}]_0 = k_2x_{eq}^2[S^0]_0 \tag{11}$$

$$\frac{k_2}{k_1} = \frac{[MV^{2+}]_0^2[S^{2-}]_0}{x_{eq}^2[S^0]_0} \tag{12}$$

As can be seen from Table 2, the rate of a reaction between elemental sulfur and cation-radical of methylviologen is 3 orders higher than the rate of direct reaction. The value of k_1 can be calculated separatedly for initial stage of catalytic reduction of MV^{2+} (first 4–5 min), when the contribution of the reverse reaction is negligibly small, i.e. at $k_1[MV^{2+}]_0[S^{2-}]_0 \gg k_2x^2[S^0]_0$. Using calculated in that way values of k_2/k_1 and k_1 we determined the rate constant of a reverse reaction k_2 (see Table 2).

3.3. Catalytic reduction of silver cations over Ag_2S nanoparticles

Upon addition of hydroquinone to a solution containing silver nitrate and PVA, the mixture becomes pale-grey coloured and a new wide band with a maximum around 420 nm appears in its absorption spectrum (Fig. 5a). This

Table 2
Kinetic parameters of the catalytic reduction of methylviologen bication

$[S^0]_0 \times 10^3$ (M)	$x_{eq} \times 10^5$ (M)	$K \times 10^5$	$k_2/k_1 \times 10^{-3}$	$k_1 \times 10^{-2}$ ($M^{-1}\ s^{-1}$)	$k_2 \times 10^{-4}$ ($M^{-1}\ s^{-1}$)
2.5	5.0	1.3	1.4	2.0	7.0
4.0	4.6	1.1	1.2	2.0	6.0
5.0	4.2	0.8	1.1	1.9	6.0
8.0	3.0	0.3	1.3	2.0	6.5
Average				2.0	6.4

Notes: $[Ag_2S] = 5 \times 10^{-4}$ M, $[Na_2S] = 1 \times 10^{-2}$ M, $[MV^{2+}] = 1 \times 10^{-3}$ M.

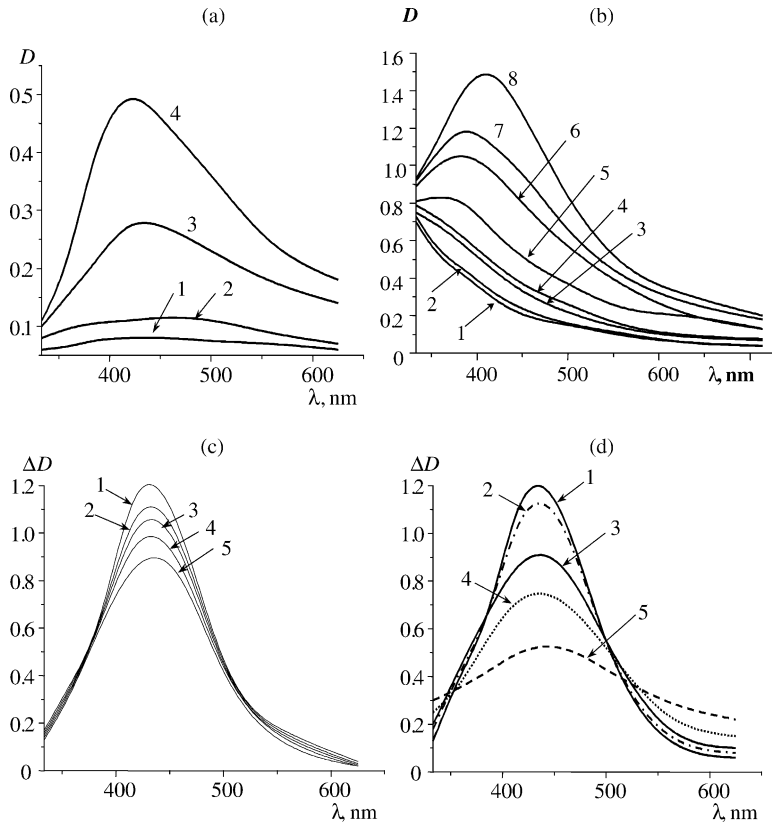

Fig. 5. (a) Temporal evolution of absorption spectra of solutions containing 2.5 mass% of PVA, $[Ag^+] = 5 \times 10^{-4}$ M, $[C_6H_4O_2] = 5 \times 10^{-4}$ M. Duration of ageing of solutions is 20 min (1), 1.5 h (2), 4 h (3), 21 h (4). (b) Temporal evolution of absorption spectrum of PVA-stabilized (2.5 mass%) colloidal Ag_2S solution (5×10^{-4} M) after an addition of $AgNO_3$ (1×10^{-4} M) and Na_2SO_3 (1×10^{-2} M): (1) initial spectrum, (2) after an addition of $AgNO_3$, (3–8) solution 2 after an addition of Na_2SO_3 (duration of the ageing of solutions is (3) 0 min, (4) 30 min, (5) 60 min, (6) 90 min, (7) 120 min, (8) 200 min). (c and d) Effect of nucleophilic agents: J^- (c) and HS^- (d) upon the parameters of plasmon resonance bands of silver. In case (c): (1) before an addition of nucleophilic agent, (2) in the presence of 1×10^{-3} M KJ, (3) solution 2 in 15 min, (4) the same at [KJ] = 1×10^{-2} M, (5) solution 4 in 75 min. In case (d): (1) before an addition of nucleophilic agent, (2 and 3) after an addition of 1×10^{-4} and 5×10^{-4} M Na_2S correspondingly, (4) solution 3 in 15 min, (5) in the presence of 1.5×10^{-3} M Na_2S, (6) solution 5 in 15 min. Spectra in (a) were registered relatively to blank PVA solution, spectra in (b–d) relatively to the solutions containing the stabilizer and 2.5×10^{-4} M Ag_2S.

change in the absorbance is caused by the reduction of Ag^+ ions [3] and simultaneous stabilization of growing colloidal particles of silver $(Ag^0)_n$ by PVA macromolecules. Similar effects can be observed in solutions containing silver sulfide nanoparticles, but in this case reduction proceeds with greater rate, distinctly prononced absorption band at 420 nm appearing at once after the mixing of reagents. The ability of Ag_2S nanoparticles to catalyze Ag^+ reduction is much more pronounced in solutions containing another reducing agent—sodium sulfite (Fig. 5b), which in the absence of Ag_2S nanoparticles very slowly reduces silver cations. It was found that in absorption spectra of solutions containing $AgNO_3$, Na_2SO_3 and a stabilizer at room temperature there are no visible changes during at least 2–3 h even at 100–500-fold excess of a reductant, whereas in the presence of colloidal Ag_2S particles absorption band of colloidal silver appears in 10–20 min after the mixing of reagents. Evolution of the absorption band of a product of silver ions reduction both by hydroquinone and sodium sulfide is not accompanied with a change in the parameters of the absorbance band of silver sulfide nanoparticles indicating that the latter are not consumed in the reaction.

According to the optics of ultradispersed metals (see, for example, [20,21]), light absorption by silver nanoparticles can in principle result in electronic transitions of three different types. First of them—low-energy intraband transitions between occupied and vacant 5sp-orbitals. They occur with the participation of phonons and do not contribute substantially in the absorbance of metal nanoparticles in the visible spectral domain. The second type is transitions from occupied 4d to vacant 5sp-levels. Absorption bands corresponding to such transitions have high intensity and are usually located in UV-region at $\lambda < 320$ nm. Transitions of third type which can not be observed for individual atoms or bulk crystals of a metal, results from collective resonance excitation of conductivity electrons within the surface layer of metal nanoparticles in the electromagnetic field of the light wave of a certain frequency. Resonances of that kind are called plasmon resonances or surface plasmons, while corresponding absorption bands are referred as plasmon absorption bands.

The existance of plasmon resonance results from quantum-mechanical description of collective electron motion. At the same time plasmon resonance and related optical properties of metal nanoparticles can be satisfactorily described by Mie theory based of the conceptions of classical electrodynamics [2,20,22].

Plasmon absorption bands of very small silver particles are located in near UV domain, while at an increase in the size of the particles maximum of plasmon band shifts to the long-wave section of the spectrum. Thus, for example, in the presence of various stabilizers spherical particles of different size (d) can be obtained with plasmon resonance at λ_{max} = 380 nm (d = 1–10 nm) [3,23], 395 nm (d = 5–20 nm) [3], 405 nm (d = 15 nm), 420 nm (d = 22 nm) [24], 425 nm (d = 40 nm) [23]. Position of the maximum of plasmon absorption band is affected not only by the size of silver particles but also by their shape, adsorption of molecules and ions of various nature on the surface of the metal, interaction with a substrate, formation of dimers (polymers) with electroconductive bridges or aggregates, in particular, fractal clusters and other [2,3,22,25–30].

Position of the maximum of plasmon absorption band of metal nanoparticles (λ_{max}) depends on the optical properties of dispersive medium and a metal as well as on the density of free electrons in metal nanoparticles (N_e) and can be calculated, according to Mie theory [20], with the use of the following basic expression:

$$\lambda_{max}^2 = \frac{(2\pi c)^2 m_e(\varepsilon_0 + 2n_0^2)}{4\pi^2 N_e} \quad (13)$$

where c is the light velocity in vacuum (m s^{-1}), m_e, e the rest mass and charge of electron (in kg and K), ε_0 a component of dielectric constant of a metal independent of light wavelength,n_0 the refraction index of dispersive medium.

Another important characteristic of a plasmon band—its half-width on half-height in maximum (w) also depends on N_e and is inversely proportional to the size of metal particles:

$$w = \frac{(\varepsilon_0 + 2n_0^2)cm_e V_F}{2N_e e^2 R} \quad (14)$$

where V_F is the velocity of electrons on Fermi level (m s^{-1}) which is equal to 1.4 × 10^6 m s^{-1} for silver [20]; 2R the diameter of metal nanoparticles.

Combining Eqs. (13) and (14) we can obtain an expression for the estimation of R basing only on the parameters of plasmon absorption band, i.e. the values of λ_{max} and w:

$$R = \frac{\lambda_{max}^2 V_F}{2\pi c w} \quad (15)$$

The values of R calculated with the use of the expression (15) should be considered as estimate, since this expression leaves out of account a number of the properties of real colloidal solution of a metal, in particular, size distribution of metal particles contributing to experimental values of w, as well as the effect of the adsorption of substrates with nucleophilic or electrophilic nature on the surface of metal nanoparticles which can alter the density of electron gas on the surface of particles, i.e. the value of N_e and, as a consequence, position of the maximum and width of a plasmon band.

Parameters of the absorption spectra of the products of Ag^+ catalytic reduction correspond well to disscussed above characteristics of absorption spectra of metallic silver nanoparticles. Indeed, in the course of silver reduction there appears additional absorbance at λ < 310 nm which can be attributed to electronic 4d → 5sp transitions, while in the domain of 330–700 nm (Fig. 5a and b) forms an absorption band with high intensity peculiar to plasmon resonance bands. Additional confirmations of the fact that absorption band of the products of catalytic reduction of Ag^+ are plasmon resonance bands of nanometer silver particles were supplied by the investigation of the effect of I^- and HS^- ions, having nucleophilic properties, on the parameters of these bands. It is known [20,21,31], that on the surface of metallic silver are always present unsaturated valencies which can accept electronic density from nucleophilic agents. This results in chemosorption of the latters accompanied with a shift in Fermi energy of a metal to more negative values and subsequent decrease in the intensity of plasmon resonance band. As can be seen from Fig. 5c, addition of KI to the reacting mixture actually induces a fall of the intensity of the absorption band of the reduction product which is the more prononced the higher concentration of I^- is. In the presence of HS^- anions (Fig. 5d), which have stronger nucleophilic properties as compared with iodide, one can observe noticeably greater decrease in the intensity of silver plasmon band and besides some widening of the absorption band, the last being in accordance with the properties of plasmon resonance absorption [20,31,32].

Accelerating effect of Ag_2S nanoparticles on the process of the formation of metallic silver is apparently based on the fact that the reduction of silver cations to atomic metal which is an initial stage of the reduction, proceeds on the surface of semiconductor nanoparticles. In the absence of such surface necessary for the adsorption both of Ag^+ and atomic silver and possibly also reducing agents (HSO_3^-, SO_3^{2-}, $C_6H_4(OH)O^-$, $C_6H_4O_2^{2-}$), on the initial stage form apparently corresponding salts, whose further redox-transformations are hampered. Thus, at the reduction of Ag^+ by hydroquinone in the absence of Ag_2S, right away after the mixing of reagents we observed an increase in optical density within the wide spectral range of 330–700 nm (Fig. 5a) caused, as we suppose, by visually detected turbidity of the solutions in the results of the formation of poorly soluble salts—$C_6H_4(OH)OAg$ and (or) $C_6H_4O_2Ag_2$. Growth of the intensity of plasmon resonance absorption band in the spectra of such solutions developed slowly (Fig. 6, curve 1). In contrast to this, in the presence of Ag_2S nanoparticles the process occurs with comparatively high rate and then, with a decrease in Ag^+ concentration, gradually slows down and comes to the end within 4–5 h (Fig. 6, curves 2 and 3).

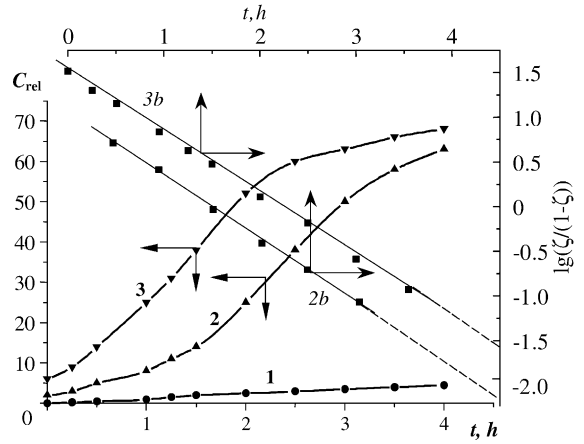

Fig. 6. Kinetics of the formation of Ag^+ reduction products at the interaction of 1×10^{-4} M $AgNO_3$ and 1×10^{-2} M Na_2SO_3: (1) in the absence of the catalyst, (2) in colloidal solution of silver sulfide at $[Ag_2S] = 5 \times 10^{-4}$ M, (3) at $[Ag_2S] = 1 \times 10^{-3}$ M (concentration of reduction products is expressed in relative units proportional to optical density of a solution at 420 nm); (2b and 3b) anamorphosis of curves (2) and (3) correspondingly in coordinates $\lg(\xi/(1-\xi)) - t$.

Two peculiarities of the catalysis of silver reduction by Ag_2S nanoparticles draw special attention. First of them consists in the high sensitivity of Ag^+ reduction to the presence of very small quantities of Ag_2S. Thus, without the catalyst at the reduction of Ag^+ by sodium sulfite at 25 °C, $[AgNO_3] = 5 \times 10^{-4}$ M, $[Na_2SO_3] = 1 \times 10^{-2}$ M and [PVA] = 2.5 wt.% we did not observe the formation of plasmon band in absorption spectra in the course of 2 h, whereas in the presence of 1×10^{-5} M Ag_2S with E_g = 1.62 eV it appears and reaches substantial intensity already in the first 15 min of the catalytic reaction. Moreover, even at $[Ag_2S] = 1 \times 10^{-6}$ M no longer than in 30 min after the mixing of reagents we observed an increase in the optical density of a solution in the spectral area corresponding to the maximum of plasmon band and within 60 min formation of plasmon absorbance band was practically finished.

The second peculiarity of the growth of silver nanoparticles consists in the autocatalytic nature of this process (Fig. 6, curves 2 and 3), the fact indicating that a product of the reduction (apparently, silver nanoparticles) can act as a catalyst. Actually, it is well known that Ag clusters forming on the surface of microcrystallites of silver halides at the exposure of photomaterials can catalyze further reduction of Ag^+ in the process of image development [13]. On the other hand, colloidal silver particles can adsorb Ag^+, Cd^{2+}, Ni^{2+}, Hg^{2+} and other ions with partial shift of electronic density from Ag particles to the ions resulting in the facilitation of the reduction of the latters [20,21]. In particular, adsorbed Hg^{2+} ions can be reduced to Hg^0 even without special additions of a reductant due to silver oxidation, while Cd^{2+} ions can be converted into metallic cadmium via photochemical process on the surface of $(Ag)_n$ particles [20,21,33]. With these facts in mind we concluded that auto-acceleration of catalytic Ag^+ reduction (Fig. 6, curves 2 and 3) is caused by the formation of additional catalyst—Ag^0 particles growing on the surface of Ag_2S.

3.4. Influence of the conditions of catalytic synthesis on plasmon resonance of silver nanoparticles

3.4.1. Concentration of silver sulfide

In a series of experiments performed to elucidate an effect of Ag_2S concentration on Ag^+ reduction rate we used mixtures containing the same stabilizer (2.5% PVA) and equal concentrations of reactants ($[AgNO_3] = 5 \times 10^{-4}$ M, $[Na_2SO_3] = 1 \times 10^{-2}$ M). In solutions containing silver sulfide nanoparticles (at $[Ag_2S] = 1 \times 10^{-6}$ M) in 30 min after the mixing of reagents we observed the rise of the absorbance at λ = 400–500 nm and in 2 h wide plasmon band having maximum at 450 nm (Fig. 7a). In 24 h reaction comes to the end

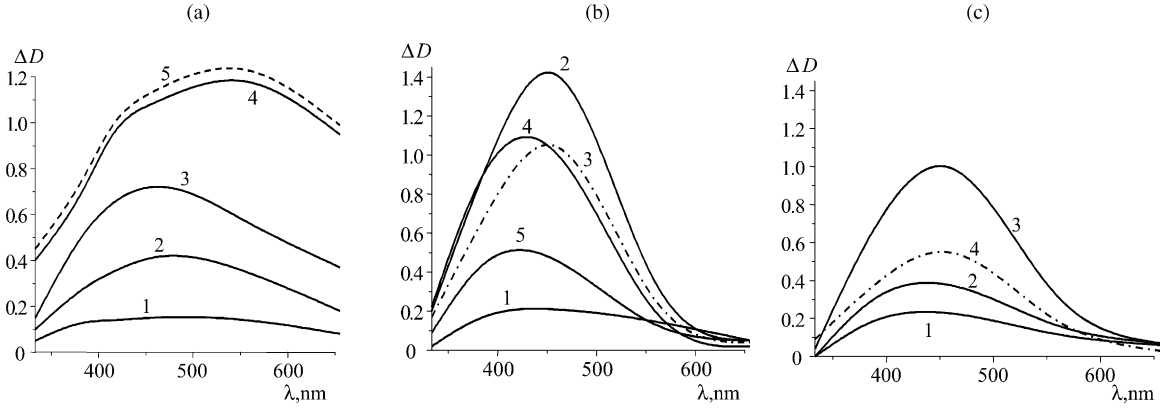

Fig. 7. Effect of molar Ag_2S and Ag^+ concentration on the parameters of absorption bands of reduction products (all spectra were recorded relatively to the reference solutions of Ag_2S): $[AgNO_3] = 5 \times 10^{-4}$ M, $[Na_2SO_3] = 1 \times 10^{-2}$ M; (a) $[Ag_2S] = 1 \times 10^{-6}$ M, spectra 1–5 were registered at τ = 0.5, 2, 3, 24 and 45 h correspondingly, l = 3.0 cm (curves 1–3), l = 1.0 cm (curves 4 and 5); (b) absorption spectra were recorded at τ = 1 h with $[Ag_2S] = 1 \times 10^{-6}$ (1), 1×10^{-5} (2), 5×10^{-5} (3), 2.5×10^{-4} (4) and 3×10^{-3} M (5), l = 3.0 (1–2), 2.0 (3), 0.3 (4) and 0.1 cm (5); (c) absorption spectra recorded in solutions with $[Ag_2S] = 2.5 \times 10^{-4}$ M, $[Na_2SO_3] = 1 \times 10^{-2}$ M at $AgNO_3$ concentrations: (1) 5×10^{-5}, (2) 1×10^{-4}, (3) 2.5×10^{-4}, (4) 5×10^{-4} M, all solutions were kept for 4 h; in case of (1–3) l = 0.5 cm, (4) l = 0.1 cm.

and at further storage the absorption spectrum of a solution with λ_{max} = 588 nm and a shoulder at 450 nm does not change (Fig. 7a, curves 4 and 5). At an increase in the concentration of catalyst in the range of 1×10^{-6} to 1×10^{-3} M the rate of catalytic reaction grows while the maximum of plasmon bands shifts in the short-wave side of the spectrum (Fig. 7b). Solutions with 1×10^{-6}, 1×10^{-5}, 5×10^{-5}, 2.5×10^{-4} and 1×10^{-3} M of Ag_2S have plasmon resonance with the maxima correspondingly at 445, 440, 435, 425 and 415 nm.

3.4.2. Concentration of Ag^+

An increase in $AgNO_3$ concentration at constant concentrations of Na_2SO_3 and Ag_2S leads to an increase in the rate of silver reduction and small hypsochromic shift of the maximum of plasmon bands. As can be seen in Fig. 7c, in 4 h after the mixing of reagents in the solution with $[AgNO_3] = 5 \times 10^{-4}$ M we observed 30 nm hypsochromic shift of Ag plasmon band as compared to the solution with $[AgNO_3] = 5 \times 10^{-5}$ M.

3.4.3. Size and stabilization of Ag_2S nanoparticles

The effect of these factors on the catalytic reduction of Ag^+ was investigated in two series of experiments. One of them was performed with Ag_2S nanoparticles having E_g = 1.4 eV and synthesized in aqueous solution without stabilizers as well as smaller nanoparticles synthesized in the presence of PVA (E_g = 1.6 eV) or gelatine (E_g = 1.7 eV). Different nature of spectral transformations progressing in the presence of these catalysts can be seen from the comparison of Fig. 8a–c. Product of catalytic reaction with the participation of the smallest gelatine-stabilized Ag_2S nanoparticles has plasmon band with the maximum at 410 nm (Fig. 8a, curve 1). In the presence of bigger colloidal particles of silver sulfide stabilized with PVA silver particles have plasmon band with the maximum at 425 nm (Fig. 8a, curve 2). With the use of Eq. (15) it can be shown that in case of gelatine-stabilized Ag_2S nanoparticles average size of Ag nanoparticles is 3.5–4.0 nm, whereas in the presence of PVA-stabilized Ag_2S nanoparticles the average size of Ag particles amounts to 5.0–5.5 nm. Ag^+ reduction catalyzed by non-stabilized Ag_2S nanoparticles with E_g = 1.4 eV has two substantial distictions. First, it has much greater rate as compared with the polymer-stabilized solutions. Broad absorption band of silver with indistinct maximum at 450 nm appears straight away after the mixing of reagents. Second, in the course of the reduction we observed considerable growth of the absorbance in the long-wave spectral domain and much more prononced shift of the maximum of the plasmon band (Fig. 8a, curve 3).

In the second series of experiments we used Ag_2S nanoparticles synthesized in aqueous solutions without polymers and then stabilized via an addition of PVA or gelatine. Spectral changes observed in these solutions are shown in Fig. 8b and c. It should be noticed that molar concentrations of reagents and colloidal catalyst were kept the same as in the first series of experiments discussed above (Fig. 8a). Distinction between the two series of experiments consists in the characteristics of Ag_2S nanoparticles – in the first case we used Ag_2S nanoparticles with E_g = 1.6 and 1.7 eV, whereas in the second – with $E_g \sim 1.4$ eV. As can be seen from the Fig. 8a, slight effect of an increase in the average size of Ag_2S nanoparticles on the position and the shape of absorption bands of the products of Ag^+ reduction (some widening of the band and shift of the maximum to 435 nm) could not be compared with strong effect of the presence (Fig. 8a) or the absence (Fig. 8b and c) of a stabilizer as well as its nature. Thus, oppositely to the solutions containing PVA and Ag_2S nanoparticles with $E_g \sim 1.4$ eV, catalytic reduction in colloidal solutions of Ag_2S containing gelatine gives the products having two overlapping band with the maxima at 415 and 510 nm (Fig. 8c).

It should be noted that colloidal Ag_2S particles both catalyze the reduction of Ag^+ by sodium sulfite and stabilize

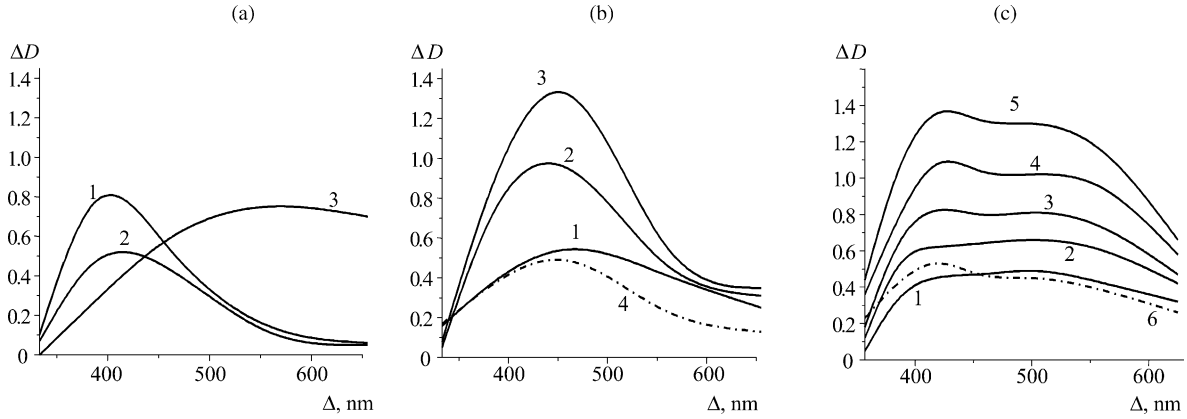

Fig. 8. Effect of the stabilization method and size of colloidal particles of the catalyst on the absorption spectra of Ag^+ reduction products ($[AgNO_3] = 5 \times 10^{-4}$ M, $[Na_2SO_3] = 1 \times 10^{-2}$ M, $[Ag_2S] = 2.5 \times 10^{-4}$ M; all spectra were registrated relatively to the solutions of silver sulfide with $[Ag_2S] = 2.5 \times 10^{-4}$ M): (a) spectra of gelatine-stabilized solutions (1), l = 0.5 cm, PVA-stabilized solutions (2), l = 0.1 cm, non-stabilized solutions (3), l = 0.5 cm; (b) solutions of non-stabilized Ag_2S nanoparticles with an addition of PVA, τ: (1) 30 min, (2) 45 min, (3) 60 min (l = 0.5 cm), (4) 21 h (l = 0.1 cm); (0) solution (c) with an addition of gelatine τ: (1) 45 min, (2) 60 min, (3) 75 min, (4) 90 min, (5) 2 h, (6) 24 h, l = 0.5 cm (1–5) and l = 0.1 cm (6).

forming particles of metallic silver. It was shown that the mixing of reagents in the presence of non-stabilized Ag_2S nanoparticles leads to the formation of transparent solutions with silver plasmon bands and prolonged aggregative stability while the same operation performed in the absence of colloidal Ag_2S results in the precipitation of silver sulfite. It indicates that Ag nanoparticles forming on the surface of the catalyst do not diffuse in the bulk of a solution but remain anchored to the surface of the semiconductor. The last fact can, as it was noticed before, affect some parameters of plasmon resonance of silver nanoparticles. However, the principle cause of the alteration of the parameters of plasmon band of Ag nanoparticles is, in our opinion, a change in the size of metal particles. Let us enumerate arguments in favour of this suggestion: (i) in every case in the conditions of the reaction promoting an enlargement of Ag_2S particles bathochromic shift of the maximum of plasmon band is observed (see Figs. 7 and 8); (ii) at a decrease in Ag_2S concentration a number of surface catalytic centers also decreases. So at constant concentrations of reagents on each particle of silver sulfide bigger silver particles are formed and the maximum of plasmon band, as can be seen from Fig. 7, shifts to longer wavelengths; (iii) an increase in $[Ag^+]/[Ag_2S]$ ratio should lead to the formation of bigger Ag particles (since the same quantity of catalytic centers takes part in the reduction of Ag^+ ions) and consequently should cause bathochromic shift of the maximum of plasmon band. As can be seen in Fig. 7c, an increase in Ag^+ concentration at $[Ag_2S]$ = constant actually causes a shift in the position of the absorption band of metallic silver; (iv) the same result can be achieved when we use bigger particles of the catalyst at its constant molar concentration, the fact equal to a decrease in the quantity of catalytic centers (Fig. 8a). The position of plasmon band of the forming silver nanoparticles is strongly affected in some unclear way the nature of a stabilizer. Thus, in solutions containing gelatine and separatedly synthesized non-stabilized Ag_2S nanoparticles, at the reduction of Ag^+ we observed two absorption bands (see Fig. 8c), whereas in the presence of PVA only one band (Fig. 8b).

3.4.4. A mechanism of catalytic action of Ag_2S nanoparticles in Ag^+ reduction

In PVA solutions containing silver nitrate and sodium sulfite, visible changes indicating on the formation of Ag^0 nanoparticles can be observed only in a few hour's time after reagents mixing (Fig. 5a). This is in good agreement with the well-known fact that metals deposition from solutions in the absence of catalysts or adsorbents is usually hindered [20] since "free" metal atoms forming on the initial stages of reduction are strong reductants and readily undergo oxidation [3,34,35]. Redox-potential of the couple Ag^+–Ag ($E^0_{Ag^+/Ag}$) is very high (−1.8 V versus NHE [20]) due to the presence of unpaired electron on the outer s-orbital of Ag atom (configuration $4d^{10}5s^1$). At the formation of $Ag_2{}^+$ cluster this potential drops almost to zero and at further nucleation approaches oscillatory to the electrode potential of bulk silver (E^0 = +0.799 V [36]). Partial compensation of unpaired electron through adsorbtive interactions can also shift the redox-potential of silver atoms to more positive values [3,34] and facilitate in that way reduction of Ag^+. It appears that in the presence of sodium sulfite having less negative redox-potential than −1.8 V (E^0 = −0.93 V at pH > 7 [36]), in the process of the reduction participate at first only Ag^+ adsorbed on the walls of the reactor and possibly on colloidal Ag_2SO_3 particles. This reaction results in the formation of small clusters composed of several atoms and very small particles of metallic silver which are able to adsorb Ag^+ ions from a solution [3,35] and catalyze their reaction with a reductant with subsequent addition of atomic silver to the growing metal particle.

The principal distinction between non-catalytic reduction and catalytic reduction of silver in colloidal solutions of silver sulfide consists apparently in adsorption of Ag^+ on the surface of Ag_2S nanoparticles facilitating initial stages of reduction, i.e. formation of separate silver atoms, clusters and nuclei of silver.

One of the features of n-type semiconductors including Ag_2S [37] is the presence of electronodonor centers on the surface of semiconductor crystals [4]. These centers originate from impurities and structure defects, in particular, vacancies—oxygen vacancies in case of oxides and sulfur vacancies in case of sulfides. Donor levels of these impurities and defects are located somewhat below the edge of the conduction band. The equilibrium between these levels and the conduction band is the factor determining the nature of conductivity of given semiconductor [4]. Authors of [5] found that in case of n-TiO_2 donor defects can *spontaneously*, i.e. without the participation of a reductant, irradiation or application of a potential, reduce a number of metal ions including silver with the formation of surface atoms, clusters and, at high concentration of defects, nanoparticles of a metal. Basing on these results we suppose that upon the addition of $AgNO_3$ to a colloidal Ag_2S solution some portion of Ag^+ undergoes reduction by surface donor defects of the semiconductor. This process is thermodynamically favourable since conduction band of Ag_2S nanoparticles (and therefore donor levels) has quite substantial negative potential [1], while the potential necessary for the reduction of Ag^+, as was mentioned above, shifts substantially to positive values due to adsorption. Silver atoms transform in clusters which can act as centers for subsequent adsorption and reduction of Ag^+ ions:

$$Ag_n/Ag_2S + Ag^+ \rightarrow Ag_{n+1}{}^+/Ag_2S \quad (16)$$

$$Ag_{n+1}{}^+/Ag_2S + Red \rightarrow Ag_{n+1}/Ag_2S \text{ and so on} \quad (17)$$

where Red is a reductant.

Forming clusters and silver nanoparticles functionate as catalysts for further Ag^+ reduction and therefore the whole process of reduction has autocatalytic nature and is described by s-shaped kinetic curves (Fig. 6). Expression for the rate of autocatalytic reduction of silver can be written in the

following way:

$$\frac{d[Ag^0]}{dt} = k[Ag^+][Ag^0] \quad (18)$$

Let $x = [Ag^0] - M$, where M is the concentration of catalytic centers at the beginning of the process ($t = 0$), $\xi = x/[Ag^+]$, $\xi_0 = M/[Ag^+]$. In the systems under examination at $t = 0$ there is no metallic silver, so M value corresponds to the concentration of active centers on the surface of Ag_2S nanocrystals which can participate in the reduction of Ag^+ (donor defects). Taking $\xi_0 \ll 1$, after substitution of x, ξ and ξ_0 parameters in the Eq. (18), integration, and conversion to decimal logarithms we obtain an expression for the calculation of the quantity of reduced silver:

$$\lg\left(\frac{\xi}{1-\xi}\right) = \lg\xi_0 + 0.434k[Ag^+]t \quad (19)$$

As can be seen in Fig. 6b, kinetic curves of Ag^+ catalytic reduction can be well linearized in coordinated of the Eq. (19) $\lg(\xi/(1-\xi)) - t$. From the slope and its intersection with the axis of ordinates can be derived rate constant of silver reduction $k = 1.6 \times 10^4\ s^{-1}$ and concentration of catalytic centers on the surface of silver sulfide nanoparticles $M \approx 3 \times 10^{-6}$ M (at $[Ag_2S] = 1 \times 10^{-3}$ M) and $M \approx 3 \times 10^{-7}$ M (at $[Ag_2S] = 5 \times 10^{-4}$ M). Calculated value of rate constant of Ag^+ catalytic reduction on the surface of Ag_2S nanoparticles is close to the values usually obtained in the processes of the development of photographic images [38,39].

3.5. Photochemical activation of Ag^+ catalytic reduction in the presence of Ag_2S nanoparticles

Irradiation of the solutions containing Ag_2S nanoparticles, Ag^+ and reductants of various nature substantially accelerates the growth of absorption bands of the products of catalytic reduction. Absorption spectra of the products of catalytic reaction in solutions with different content of reactants are given in Fig. 9a–c, while kinetic curves of Ag^0 accumulation under the irradiation and in the dark are presented in Fig. 10a. Examination of the curves shows that variations in the concentrations of reagents has different effect on dark and photochemical processes. As can be seen at the comparison of the curves 2 and 3 in Fig. 10a with the corresponding curves in Fig. 6, efficiency of the catalytic process in the dark is strongly affected by Ag^+ concentration and weakly depends on the concentration of a reductant. This fact agrees well with the conception of [38,39] about the limiting role of the stage of generating of metallic catalytic centers on the surface of colloidal Ag_2S in the reduction of silver ions. Analysis of the energetics of photogenerated in Ag_2S nanoparticles charge carriers (given in details in [1]) shows that light absorption produces conduction band electrons which can reduce silver ions. Hence, at the irradiation of solutions resulting in the formation of high quantities of metallization nuclei will change reduction mechanism, the stage of primary nuclei formation will lose its limiting character and the basic influence on the catalytic reduction will exert the concentration of a reductant. Actually, as can be seen in Fig. 10a (compare curves 1 and 3), at the same concentration of $AgNO_3$ formation of Ag^0 in the solution with $[Na_2SO_3] = 5 \times 10^{-2}$ M proceeds much faster than in the solution with $[Na_2SO_3] = 1 \times 10^{-2}$ M. We observed also an increase in the rate of photochemical process at an increase in $AgNO_3$ concentration (at $[Na_2SO_3]$ = constant).

Catalytic synthesis of silver nanoparticles progresses via consecutive acts of adsorption of Ag^+ on metallic catalytic centers, its reduction and addition of Ag^0 atom to growing silver nanoparticles. One should expect that in conditions favouring to the formation of great quantity of such metallic centers (including the irradiation), catalytic reduction would results in smaller particles as compared with the reduction

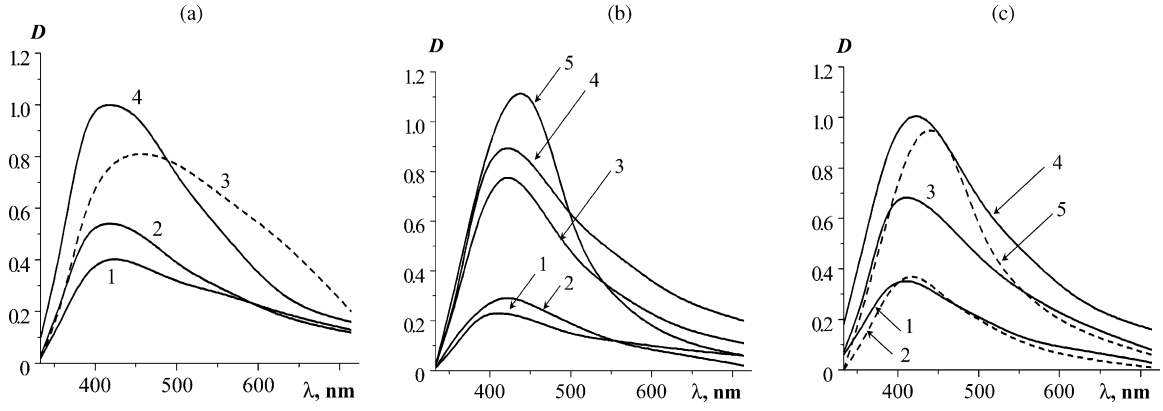

Fig. 9. (a–c) Absorption spectra of silver nanoparticles synthesized in various conditions in solutions with $[Ag_2S] = 5 \times 10^{-4}$ M. (a) Spectra of the products of reduction in irradiated solutions. Concentration of $AgNO_3$ in starting solutions: (1) 5×10^{-5}, (2) 1×10^{-4}, (4) 5×10^{-4} M, $[Na_2SO_3] = 1 \times 10^{-2}$ M. In the solution (3) $[AgNO_3] = 5 \times 10^{-5}$ M, $[Na_2SO_3] = 5 \times 10^{-2}$ M. (b and c) Spectra of silver nanoparticles synthesized in solutions with $[Na_2SO_3] = 1 \times 10^{-2}$ M and 1×10^{-4} M (b), 5×10^{-4} M $AgNO_3$ (c), in the dark during 45 min (spectra 2b and 2c), 17 h (5b) and 2 h (5c), at the stationary irradiation during 10 min (1b and 1c) and 45 min (4b and 4c), at the irradiation for 5 min with subsequent ageing for 40 min in the dark (curves 3b and 3c). Duration of the reaction in minutes: (1) 60, (2) 90, (3) 20, (4) 30, (5) 45, (6) 60, (7) 90.

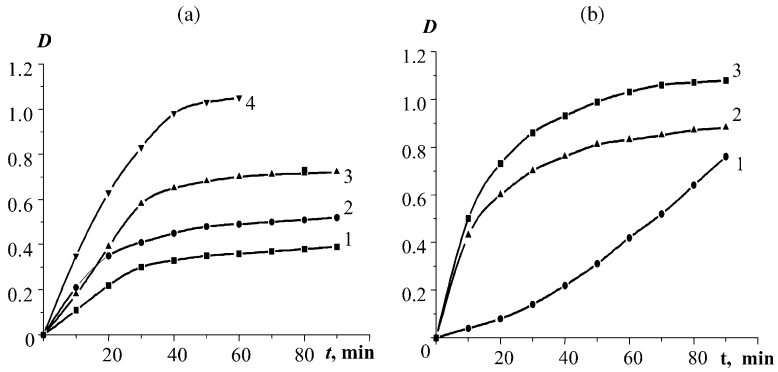

Fig. 10. (a) Evolution of plasmon resonance absorption bands of silver nanoparticles at the ageing of colloidal solutions with $[Ag_2S] = 5 \times 10^{-4}$ M under the irradiation. In the solutions (1, 2 and 4) $[Na_2SO_3] = 1 \times 10^{-2}$ M, $[AgNO_3]$ in (1) 5×10^{-5}; (2) 1×10^{-4}; (4) 5×10^{-4} M, in the solution (3) $[Na_2SO_3] = 5 \times 10^{-2}$ M, $[AgNO_3] = 5 \times 10^{-4}$ M. (b) Kinetic curves reflecting a change in the intensity of plasmon bands of silver nanoparticles at ageing of colloidal solutions with $[Ag_2S] = 5 \times 10^{-4}$ M, $[AgNO_3] = 1 \times 10^{-4}$ M and $[Na_2SO_3] = 1 \times 10^{-2}$ M in the dark (1), at the irradiation for 5 min and subsequent ageing in the dark (2), at the stationary irradiation (3).

in the dark. To verify this assumption we compared absorption spectra of the corresponding solutions after completion of Ag^+ reduction and found that at $[Ag_2S] = 5 \times 10^{-4}$ M, $[Na_2SO_3] = 1 \times 10^{-2}$ M and $[AgNO_3] = 5 \times 10^{-5}$ to 5×10^{-4} M products of the photoreaction have absorption bands with the maxima at 410–420 nm, whereas the products of the thermal process at 430–450 nm (see Fig. 9a–c). According to [20,21,30], a shift of plasmon band position to longer wavelengths can be induced by an increase in the size of Ag nanoparticles. The same character of temporal transformations of absorption bands of the products of photochemical and dark reduction indicates that these products have the same chemical nature (i.e. in both cases it is nanoparticulate silver on the surface of colloidal Ag_2S nanoparticles) but differ in the quantity of silver atoms per particle. As can be seen in Fig. 9b and c, after 10 min irradiation of solutions with the concentrations of $AgNO_3$ equal to 1×10^{-4} and 5×10^{-4} M, the maxima of plasmon band are located correspondingly at 405 and 410 nm (spectra 1), while after 45 min irradiation at 415 and 420 nm (spectra 4). Similar shifts can be also observed at the ageing of colloidal solutions in the dark. Comparison of the spectra 2 and 4 in Fig. 9b shows that the absorption bands of the products of photochemical and thermal (dark) reduction have identical maxima but strongly differ in the intensity. This fact can be naturally explained in the following way. At low content of metallization nuclei on the surface of Ag_2S colloids kept in the dark as compared with illuminated colloids quantity of Ag nanoparticles is also low. At further ageing of these solutions catalytic reduction goes on, the size of Ag nanoparticles grows and the intensity of silver plasmon band increases so its maximum shifts to 435–440 nm (Fig. 9b and c, curves 2 and 5). Additional argumentation in favour of the proposed interpretation can be extracted from the experiments where solutions were exposed to short-time irradiation and then aged in the dark. As can be seen in Fig. 10b, generation of a substantial quantity of catalytic centers in the course of first 5 min of irradiation results in the acceleration of the subsequent dark reduction. In this case the rate of dark reduction is almost equal to the rate of photochemical process at stationary irradiation.

It should be noted that at the same composition of reacting mixtures silver deposition under the irradiation and in the dark results in the formation of Ag nanoparticles having absorption bands which differ not only in the position of the maximum but also in the shape (see Fig. 9b and c, curves 4 and 5). The last fact can be explained by diverse effect of semiconductor matrix on the silver nanoparticles forming in the course of the dark and photochemical processes. The nature of this effect is usually determined by the nature of electronic processes in the coupled “metal-semiconductor” system. It is well known (see for example [40]), that at the establishment of a contact between these materials due to the difference in their work functions there always is some migration of electrons from a n-type semiconductor to a metal, which can affect the electronic properties of both components. In [5,41,42] such reciprocal influence was observed at the photodeposition of silver on the surface of ZnO and TiO_2 [5]. In the system under investigation at dark reduction metallization nuclei form apparently as a result of the interaction of Ag^+ ions with donor defects in the surface of Ag_2S nanoparticles. Surface defect are oxidized by Ag^+ ions, growing Ag nanoparticles do not have electric contact with the substrate (Ag_2S) and the semiconductor does not virtually affect optical properties of metal nanoparticles [5]. On the contrary, under the irradiation the greater part of nuclei is generated in photocatalytic process which does not chemically alter the surface of silver sulfide nanoparticles. As a result, a contact between semiconductor and growing metal particles would remain undisturbed and the components of such binary system can interact. Hence, silver sulfide affects optical properties of Ag nanoparticles similarly to nucleophilic agents [20,21], i.e. induces a widening of the plasmon bands and a decrease in their intensity (Fig. 9b and c, curves 4 and 5).

4. Conclusions

In the present paper we discussed the nature of primary photoprocesses and quantum confinement effects in silver sulfide nanoparticles, determined types and energies of optical transitions responsible for light absorption by Ag_2S nanoparticles.

Catalytic properties of Ag_2S nanoparticles in the process of methylviologen reduction by sodium sulfide were investigated. It was shown that the catalytic reaction is an equilibrium one due to a reverse reaction between the products of catalytic process, elemental sulfur (polysulfide ions) and methylviologen cation-radical.

It was found that Ag_2S nanoparticles act as catalysts of Ag^+ ions reduction to nanoparticulate metallic silver by reductants of various nature. The effect of the conditions of catalytic reduction of silver ions on the shape and intensity of plasmon bands of nanoparticulate silver was investigated. A scheme of the mechanism of catalytic Ag^+ reduction was discussed. It was shown that the irradiation of solutions containing Ag_2S nanoparticles, Ag^+ ions and a reductant with the light corresponding to the absorption band of silver sulfide leads to an increase in the rate of silver reduction, a change in the kinetics of this process as well as parameters of plasmon resonance bands of silver nanoparticles forming in the course of catalytic reduction. A plausible mechanism of photochemical activation of catalytic Ag^+ reduction with the participation of Ag_2S nanoparticles was proposed.

In conclusion it should be noted that the control over the synthesis of silver nanoparticles through variation of its conditions to obtain nanoparticulate silver with desired electronic and optical properties is very important because of the capability of the development of various functional materials based on the $(Ag^0)_n/Ag_2S$ composite nanoparticles.

References

[1] A.I. Kryukov, S.Ya. Kuchmii, V.D. Pokhodenko, Theor. Exp. Chem. 36 (2000) 69.
[2] V.I. Roldugin, Russ. Chem. Rev. 69 (2000) 899.
[3] A.D. Pomogailo, A.S. Rosenberg, I.E. Uflyand, Metal Nanoparticles in Polymers, Chemistry, Moscow, 2000.
[4] V.Ya. Gurevich, Yu.V. Pleskov, Photoelectrochemistry of Semiconductors, Nauka, Moscow, 1983.
[5] A.I. Kulak, Electrochemistry of Semiconductor Heterostructures, Universitetskoye, Minsk, 1986.
[6] Y. Wang, N. Herron, J. Phys. Chem. 95 (1991) 525.
[7] J.Z. Zhang, J. Phys. Chem. B 104 (2000) 7239.
[8] D. Beydoun, R. Amal, G. Low, S. McEvoy, J. Nanoparticles Res. 1 (1999) 439.
[9] R.F. Khairutdinov, Russ. Chem. Rev. 67 (1998) 125.
[10] A.I. Kryukov, S.Ya. Kuchmii, V.D. Pokhodenko, Theor. Exp. Chem. 33 (1997) 306.
[11] P. Hoyer, H. Weller, Chem. Phys. Lett. 224 (1994) 75.
[12] V.S. Arakelyan, J. Phys. Chem. (Russ.) 65 (1991) 1454.
[13] T.H. James, The Theory of the Photographic Process, Macmillan Publishing Co, New York, London, 1977.
[14] L. Spanhel, H. Weller, A. Fojtik, A. Henglein, Ber. Bunserges. Phys. Chem. 91 (1987) 88.
[15] M.Y. Han, W. Huang, C.H. Chew, et al., J. Phys. Chem. B 102 (1998) 1884.
[16] M.C. Brelle, J.Z. Zhang, L. Nguyen, R.K. Mehra, J. Phys. Chem. A 103 (1999) 10194.
[17] K. Seeger, Semiconductor Physics, Springer-Verlag, Berlin, Heidelberg, New York, London, 1991.
[18] N.B. Hannay (Ed.), Semiconductors, Reinhold Publishing, 1962.
[19] Y. Nosaka, M.A. Fox, J. Phys. Chem. 92 (1988) 1893.
[20] A. Henglein, J. Phys. Chem. 97 (1993) 5457.
[21] A. Henglein, Chem. Mater. 10 (1998) 444.
[22] U. Kreibig, M. Gartz, A. Hilger, Ber. Bunsenges. Phys. Chem. 101 (1997) 1593.
[23] A.L. Rogach, G.P. Shevchenko, Z.M. Afanas'eva, V.V. Sviridov, J. Phys. Chem. B 101 (1997) 8129.
[24] H.H. Huang, X.P. Ni, G.L. Loy, et al., Langmuir 12 (1996) 909.
[25] G.B. Sergeev, Russ. Chem. Rev. 70 (2001) 915.
[26] M.V. Kiryukhin, B.M. Sergeev, A.N. Prusov, V.G. Sergeev, Polymers (Russ.) 42B (2000) 2117.
[27] M.D. Malinsky, K.L. Kelly, G.C. Schatz, et al., J. Phys. Chem. B 105 (2001) 2343.
[28] C.L. Haynes, R.P. Van Duyne, J. Phys. Chem. B 105 (2001) 5599.
[29] W.P. McConnell, J.D. Novak, L.C. Broussean, J. Phys. Chem. B 104 (2000) 8925.
[30] M.P. Pileni, New J. Chem. (1998) 693.
[31] L. Katsikas, M. Gutierrez, A. Henglein, J. Phys. Chem. 100 (1996) 11203.
[32] A. Henglein, T. Linnert, P. Mulvaney, Ber. Bunsenges. Phys. Chem. 94 (1990) 1449.
[33] A. Henglein, Ber. Bunsenges. Phys. Chem. 101 (1997) 1562.
[34] B.G. Ershov, Russ. Chem. Rev. 66 (1997) 103.
[35] V.V. Sviridov, Non-silver Photographic Materials, Khimia, Leningrad, 1984.
[36] A.M. Sukhotin (Ed.), Reference Book of Electrochemistry, Khimia, Leningrad, 1981.
[37] P. Junod, Helv. Phys. Acta 32 (1959) 567.
[38] V.S. Kondrasheva, G.A. Nenadova, N.V. Palishkina, N.I. Savvin, V.D. Yagodovski, J. Phys. Chem. (Russ.) 65 (1991) 934.
[39] S.K. Donkpegan, V.V. Tsvetkov, V.D. Yagodovski, J. Phys. Chem. (Russ.) 72 (1998) 1820.
[40] A.L. Linsebigler, G. Lu, J.T. Yates, Chem. Rev. 95 (1995) 735.
[41] S. Chen, U. Nickel, J. Chem. Soc. Faraday Trans. 92 (1996) 1555.
[42] A.L. Stroyuk, V.V. Shvalagin, S.Ya. Kuchmii, Theor. Exp. Chem. 40 (2004) 94.